Transactions of the **14th International Conference on Structural Mechanics in Reactor Technology** (SMiRT 14), Lyon, France, August 17-22, 1997 **J02/5**

Shock loading on concrete walls : damage evaluation using hydrocodes

Lagasco F., Manfredini G.M.
D'Appolonia S.p.A., Italy

ABSTRACT: The structural resistance of reinforced concrete walls subject to shock loading can be evaluated by means of hydrocodes. From practical design experience, it is noted that monitoring relevant variables at early impact times of the numerical analyses is conducive to a sound judgement of the structural resistance. In this context, a tentative methodology for damage evaluation is presented. Simulations of a nearby high-explosive burst and of a hard missile impact are presented and their results are interpreted on the basis of the proposed methodology. Results are also compared with predictions based on experimental results.

INTRODUCTION

When reinforced concrete structures are subjected to shock loading that causes rapid and severe compression waves running through, the material locally behaves in an almost fluid-like manner. The overall geometric configuration of the structure is of secondary importance compared to the localised material response. Computer modeling requires the use of hydrocodes which comprehend finite element or finite difference formulations of the material continuum, equations for the conservation of mass, momentum and energy and realistic constitutive models.

The work presented is related to the experience gained by the use of the finite difference codes Autodyn-2D and CTH. Autodyn-2D is a two-dimensional coupled code employing Lagrangian, Eulerian and mixed processors [1]. CTH is a code developed at Sandia National Laboratories to model strong shock wave physics. It adopts an Eulerian two-step scheme: in the first step the Lagrangian calculation is performed, in the second step the distorted mesh is mapped back to the Eulerian mesh [2].

When hydrocodes are employed to model the material structural response, difficulties arise in performing numerical analyses over few milliseconds. Severe mesh distortion and tangling as well as density and pressure instabilities can force analyses to premature end. A tentative methodology for damage evaluation is proposed to overcome the problem. It includes monitoring relevant variables in the impacted zone, such as the velocity of the structural parts, the plastic strain of the steel reinforcement, and the amount of fractured concrete at early times of analysis to judge about the resistance of the wall.

1 THEORETICAL BACKGROUND

It is known that the fast dynamic loading of a shock event causes the raise and rapid propagation of compression waves with high pressure magnitude. These waves, which in case

of contact detonation can possess a velocity much higher than the sound velocity, reflect and refract when encounter a boundary. When a plane wave running through an impacted concrete section strikes the rear side boundary, it totally reflects with a 180° change in phase, i.e. a compression wave is reflected as a tension wave and combines with the tail of the compression wave to produce a net stress [3]. If the net stress exceeds the dynamic tensile strength of the material, this causes the rupture of a conical region of the rear side material and the consequent ejection of the cracked-off part at some velocity. This phenomenon, called spalling, is more evident in concrete, which is stronger in compression than in tension, but interests metals too. When the hydrostatic tension exceeds the local spall strength of metallic material, instantaneous microcracks growth and coalescence can lead to local fracture [4]. The behavior of materials is commonly quantified in hydrocodes for fast dynamics by an equation of state (EOS) governing the material volumetric behavior, a strength model describing the shear behavior and a failure model.

1.1 Equation of State

The equation of state determines the pressure in the material as a function of its density and internal energy and is typically represented by a pressure/volumetric strain relation. For concrete, the piecewise linear relation of porous materials is generally assumed (Figure 1). This diagram is equivalent to the hydrostatic part of the stress/strain relationship. Necessary input can be obtained from triaxial laboratory tests performed on concrete samples. For the reinforcement steel the dependency can be linear, i.e. purely governed by the bulk modulus, or of type " shock".

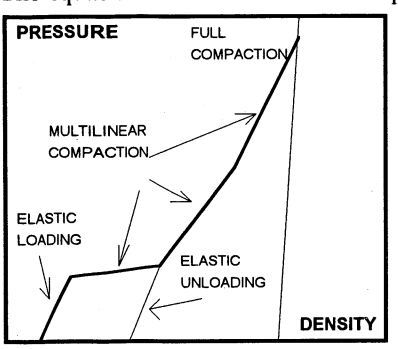

Figure 1. Equation of state for concrete

1.2 Strength model and failure criteria

The strength model defines material yielding caused by shear deformation in the material and the deviatoric stresses that shear deformation causes. Overcomes of the limits resolve in failure. For concrete, the commonly used model is represented by the pressure dependent yield surface of the Mohr-Coulomb model (Figure 2). More refined models are currently under development.

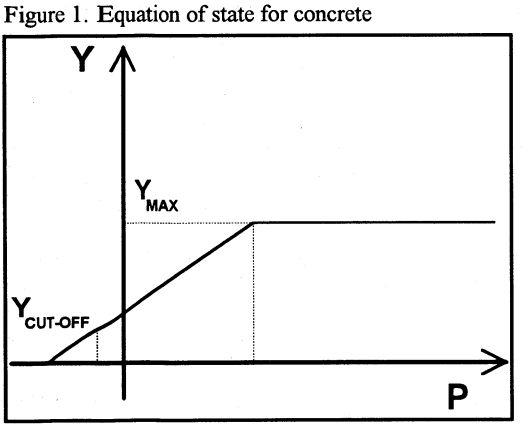

Figure 2. Mohr-Coulomb model for concrete

Provided that the concrete stress state lies beneath the failure envelope, it behaves elastically in accordance to its shear modulus. If the yield stress Y is exceeded at a certain time step, according to the following relation:

$$\frac{3}{2}\left(S_{xx}^2 + S_{yy}^2 + S_{zz}^2 + 2\,T_{xy}^2\right) \geq Y^2 \qquad (1)$$

being S_{xx}, S_{yy}, S_{tt} the components of stress deviator tensor and T_{xy} the component of the total stress tensor, the stress deviators are scaled back to the yield surface. The maximum yield strength specifies the point over which the material behaves according to the Von Mises criterion. This limit to the 3-D cone of the stress space represents a non-associated flow rule since it does not allow volume change during plastic flow. On the tensile side the simple pressure $Y_{cut\text{-}off}$ of the strength model provides a practical device to model concrete spalling. If this failure pressure is reached the material does not transmit shear stresses or tensile pressures any more.

The failure criterion for steel is usually based on the cumulated effective plastic strain defined as:

$$\varepsilon^{p}_{n+1} = \varepsilon^{p}_{n} + \frac{\sqrt{3J_2}\ Y}{3\mu} \tag{2}$$

being J_2 the second invariant of the stress tensor deviator and μ the shear modulus. A simple multiaxial strength model for steel refers to the Von Mises yield criterion which defines the relationship between yield limit and the second invariant of the deviator stress tensor as reported in Equation (1). In this case Y_{max} represents the steel yield stress in uniaxial tension. Strain rate dependent models accounting for local multiaxial stress state effects constitute an improvement of models previously described, such as the Johnson and Cook model [5]. It furnishes the Von Mises yield stress as:

$$Y = \left[A + B(\varepsilon_p)^n\right]\left[1 + C \ln \dot{\varepsilon}_p\right]\left[1 - T^m_{HOM}\right] \tag{3}$$

being A,B,C, m and n the material constants, ε_p and $\dot{\varepsilon}_p$ the equivalent plastic strain and the normalised equivalent plastic strain rate (dimensionless) respectively, and T_{HOM} the homologous temperature.

2 METHODOLOGY FOR DAMAGE EVALUATION

The proposed methodology is based on monitoring three variables throughout early impact times of numerical simulations: equivalent plastic strain, velocity of structural parts and concrete fractured area. Limit conditions for damage evaluation are detailed in the following paragraphs.

2.1 *Steel equivalent plastic strain*

The local resistance of reinforced concrete sections to shock loading is enhanced by steel reinforcement. Limits on the effective plastic strain in the steel reinforcement can be taken as an indication of failure conditions. Experimental values of dynamic strain to failure of steel rebars are seldom available, and conservatively the equivalent plastic strain corresponding to the ultimate static elongation can be taken as representative of failure. This can be accomplished by simulating a uniaxial tension test of a simple specimen subjected to a constant extension velocity consistent with the desired strain rate. The engineering strain in terms of percentile elongation at failure univocally sets limits to the equivalent plastic strain.

Equivalent plastic strain caused by severe shock loading can exceed 100% [4]. Example of a uniaxial tension test model is displayed in Figure 3.

A more refined approach is represented by the Johnson and Cook fracture model [6] which depends on five experimental parameters $D_1...D_5$. For the numerical case history presented in Section 3.2, a representative curve of fracture strain for common steel rebars is plotted in Figure 4. Fracture varies in function of a dimensionless pressure-stress ratio $\sigma^* = \frac{\sigma_m}{\bar{\sigma}}$, being σ_m the average of the three normal stresses and $\bar{\sigma}$ the Von Mises equivalent stress. This curve is constructed from the results of the uniaxial tension test simulation, neglecting strain rate and temperature effects. At high pressure-stress ratios fracture strain is limited by the minimum fracture strain at spall condition.

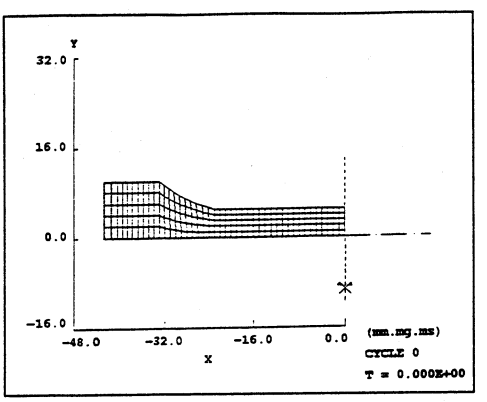

Figure 3. Numerical model of uniaxial test

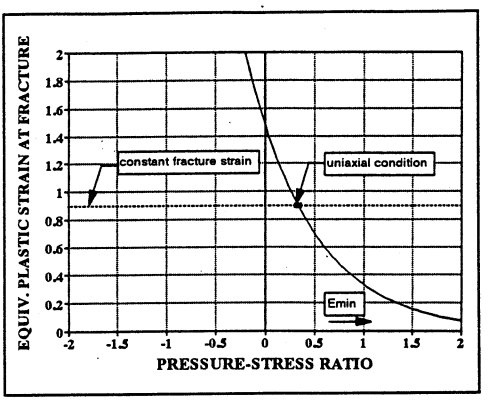

Figure 4. Fracture strain for steel rebars

2.2 *Velocity of structural parts*

The kinetic energy imparted by shock loading to structural parts is transformed into strain energy. If part of kinetic energy of structural elements remains after early times of impact, it indicates failure.

On turn, when velocities at target points are not damped by the capability of the structure of absorbing energy and maintain constant through time over a fraction of the initial velocity from the beginning of the loading time, this indicates complete structural failure, namely breaching or perforation. Nevertheless, judgement on section resistance is complemented with evaluation of fracture of steel and concrete.

2.3 *Concrete fractured area*

Fractured concrete cannot transmit stress and behaves as a mass. Damage in concrete walls caused by shock loading can be qualitatively classified by means of concrete damage categories (Figure 5).

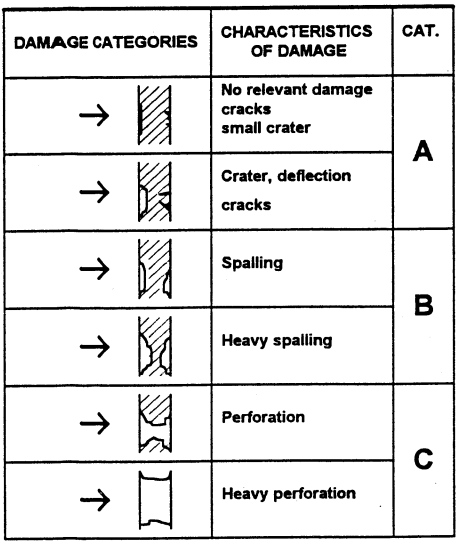

Figure 5. Damage categories

2.4 *Summary Table*

The summary table 1 can be preliminary drawn on the basis of the criteria previously described. For the condition "No Perforation" associated to concrete damage categories A and B at least one of the first two rules shall be verified. The third rule is a supplementary indication of reinforced concrete behavior.

CONDITIONS ASSOCIATED TO DAMAGE CATEGORIES	P_1	P_2	P_3
No Perforation (A, B)	< 0.1	< 1	< 1
Perforation (C)	> 0.1	> 1	1

Table 1. Damage Table

P_1 = actual velocity /maximum velocity;
P_2 = actual steel equiv. plastic strain/ultimate equiv. plastic steel strain;
P_3 = actual failed concrete thick./total thick.

3 NUMERICAL CASE HISTORIES

3.1 *Case 1, Nearby Blast*

The scenario is represented by the detonation of 100 kg of TNT nearby (15 cm standoff) a concrete wall of 0.50 m, enclosed by two steel plates of 2.5 cm at opposite sides. The axisymmetric model includes the Lagrangian subgrid of the concrete wall, two shell subgrids of the inner and outer steel plates, and an Eulerian subgrid to capture the pressure rise in air and within the TNT (Figure 6).

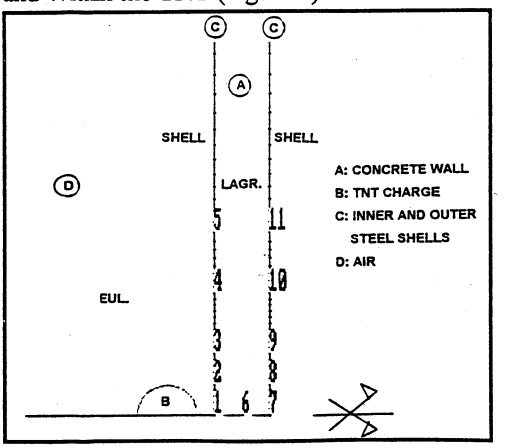

Figure 6. Model set-up for HE contact burst

The non stationary pressure pulse is applied to the concrete structure by coupling the Eulerian and Lagrangian grids. Boundary flow conditions are applied to the Euler zone to simulate outflow. The ultimate plastic strain to failure of steel shells has been set equal to 100%. Target points have been located in the Lagrangian grids to store monitored variables. The run has been prolonged up to 5 msec with time step, automatically varying, between 10^{-6} and 10^{-7} msec, on the basis of mesh dimension and pressure wave velocity. Results show a maximum pressure of the impinging wave of about 1 GPa, and lower values inside the concrete. Outer shell velocity reduces its intensity at 3 msec to a low value (Figure 7). Concrete fails in one meter radius.

The maximum plastic equivalent strain of steel is below 1.5% (Figure 8). This means that only

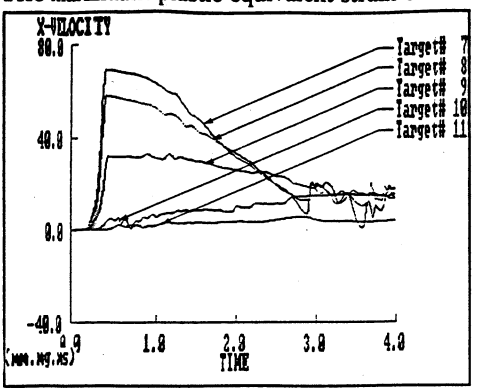

Figure 7. Velocity at target points on the outer wall surface

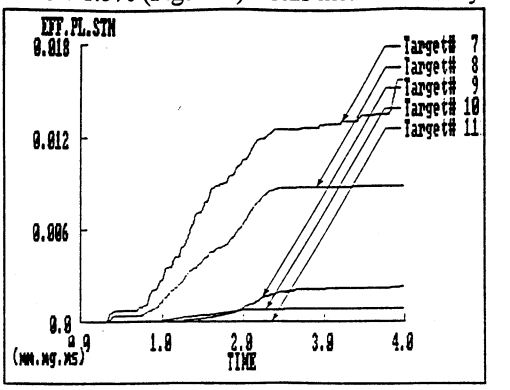

Figure 8. Equivalent plastic strain at target points on the outer wall surface

deflection and local plasticity of the two steel plates is expected. The three parameters of the damage table are 0.24, 0.015 and 1, respectively; it can be concluded that the section will not suffer perforation.

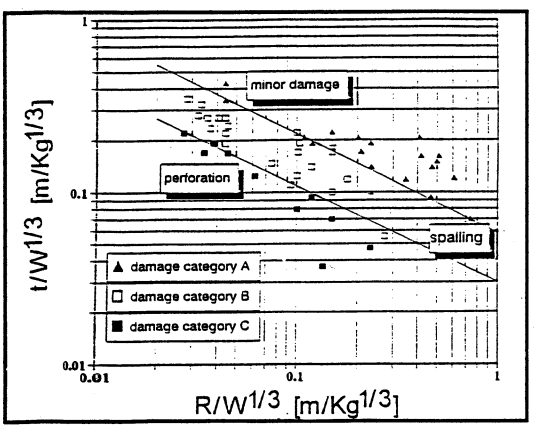

Figure 9. Experimental results of bare charges effects on reinforced concrete walls

The numerical results can be compared with experimental data available in literature [7]. In Figure 9 effects of bare charges against concrete wall are reported, with reference to damage categories. R represents the distance between wall surface and center of charge, t is the thickness of the wall and W is the charge weight.
For the current scaled distance $R/W^{1/3}$ of 0.085 and a scaled thickness $t/W^{1/3}$ equal to 0.20 (having smeared the steel plates thickness to an equivalent concrete thickness), a prediction of minor damage/spalling extent can be derived from the experimental plot (Figure 9).

3.2 Case 2, Impact of Turbine Rotor Fragment

The second application refers to the impact of a turbine rotor fragment, i.e. a 120° sector of turbine rotor weighting 11,130 Kg, which hits a containment wall at 205 m/sec. A wall thickness of 2.1 m is designed to contain the missile, on the basis of empirical formulations. The reinforcement includes an inner steel plate of 2.2 cm and bi-directional steel bars on the outer side of the containment wall, for an equivalent thickness of 1 cm. Figure 10 describes the axisymmetric scheme adopted to model the structural problem, where Lagrangian processors are used for projectile and target, while two shell elements simulate the inner steel plate and the outer reinforcing bars.

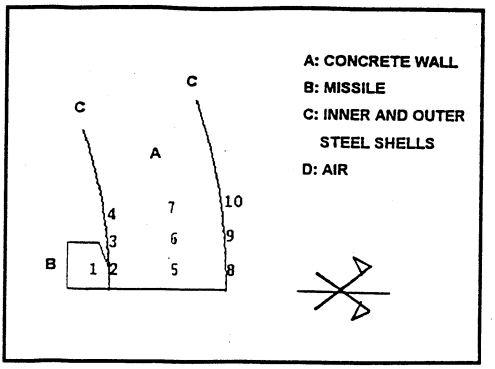

Figure 10. Model set-up for the hard missile impact

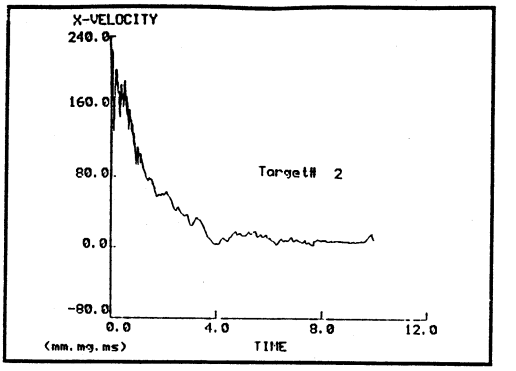

Figure 11. Velocity time history at target point 2

A sliding interface is used between the two Lagrangian grids to provide the time dependent projectile-target interaction. In this case an ultimate plastic steel strain of 90% has been numerically derived from the simulation of a uniaxial tension test. This strain corresponds to a static steel fracture strain of 20%. The peak pressure in the concrete is about 0.2 GPa. At 10 msec the fractured concrete cone is well formed and interests a radius of about 1.5 m. At the same time the target velocity has reduced from 205 m/sec to 10 m/sec while structural parts show low velocity (Figure 11). Equivalent plastic strain in the outer steel indicates failure at 5.8 msec (Figure 12). The three parameters of the damage table are 0.05, 1 and 1. These results indicate "No Perforation". Structural velocity has been damped out, the structure is at its limits of resistance. Comparison with experimental data for the specific impact scenario is reported in Figure 13.

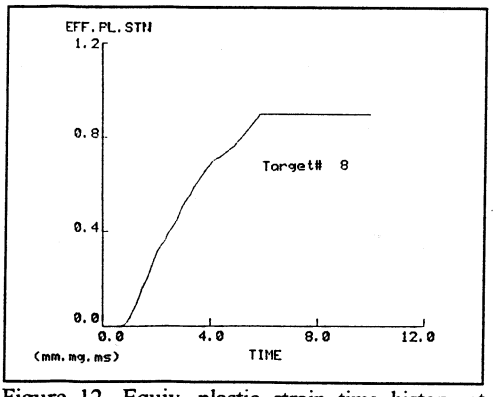

Figure 12. Equiv. plastic strain time history at target point 8

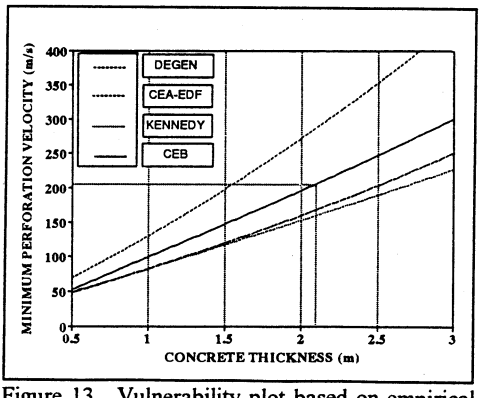

Figure 13. Vulnerability plot based on empirical formulas

In this figure empirical predictions of perforation velocity against wall thickness are given on the basis of experimental tests of turbine missiles (Degen, CEA-EDF, Kennedy, [8]) and hard missiles (CEB, [9]).

CONCLUSIONS

Experience in interpreting the results of finite difference hydrocodes applied to the structural response of reinforced concrete walls subjected to shock loading has been presented. It has been shown that monitoring variables such as velocity of structural parts, plastic strain in the reinforcement, and size of the fractured concrete area can provide sufficient indications to judge about local resistance at early times of analyses.

REFERENCES

[1] Century Dynamics, 1989, "Autodyn TM, Software for Non-Linear Dynamics, Users Manual", Oakland.

[2] McGlaun, J. M., S. L. Thompson and M. G. Elrick, 1990, "CTH: a Three-Dimensional Shock Wave Physics Code", *International Journal of Impact Engineering*, 10.

[3] Rinehart, J. S., 1975, "Stress Transients in Solids", HyperDynamic, SantaFe, NM.

[4] Zukas, J. A., 1990, "High Velocity, Impact Dynamics", John Wiley and Sons Publishers.

[5] Johnson, G. R., and W. H. Cook, 1983, "A Constitutive Model and Data for Metals Subjected to Large Strains, High Strain Rates and High Temperatures", *Proceedings of the 7th International Symposium on Ballistics*, The Hague, The Netherlands.

[6] Johnson, G. R., and W. H. Cook, 1985, "Fracture Characteristics of Three Metals Subjected to Various Strains, High Strain Rates, High Temperatures and Pressures", *Engineering Fracture Mechanics*, The Hague, The Netherlands.

[7] Hader, H., and E. Basler & Partners, 1983, "Effects of Bare and Cased Explosives Charges on Reinforced Concrete Walls", *Proceedings of the Symposium on the Interaction of Non-Nuclear Munitions with Structures*, Colorado, May.

[8] Walter, T. A. & Wolde-Tinsae, A. M. "Turbine missile perforation of reinforced concrete", *Journal of Structural Engineering*, ASCE, 1984, 110, 2439-2455.

[9] Comitè Euro-International du Beton (CEB), "Concrete Structures Under Impact and Impulsive Loading", *Bulletin d'Information*, 1988, 187.